Desalination and Water Treatment
www.deswater.com
doi: 10.1080/19443994.2015.1094420

57 (2016) 18739–18747
August

Taylor & Francis
Taylor & Francis Group

Optimization of As(V) removal using chitosan-coated bentonite from groundwater using Box–Behnken design: effects of adsorbent mass, flow rate, and initial concentration

Carlo Vic J. Arida[a], Mark Daniel G. de Luna[b], Cybelle Morales Futalan[c], Meng-Wei Wan[d,*]

[a]*Environmental Engineering Unit, University of the Philippines-Diliman, Quezon City 1800, Philippines, email: cvjarida@rocketmail.com*
[b]*Department of Chemical Engineering, University of the Philippines-Diliman, Quezon City 1800, Philippines, email: mgdeluna@gmail.com*
[c]*Operations Department, Frontier Oil Corporation, Makati City 1229, Philippines, email: cmfutalan@gmail.com*
[d]*Department of Environmental Resources Management, Chia Nan University of Pharmacy and Science, Tainan 71710, Taiwan, Tel. +886 6 266 0615; Fax: +886 6 213 1291; email: peterwan@mail.cnu.edu.tw*

Received 3 February 2015; Accepted 4 September 2015

ABSTRACT

This work focused on the removal of As(V) using chitosan-coated bentonite (CCB) from groundwater in a fixed-bed system. Thomas and Yoon–Nelson models were applied to the experimental data in order to predict breakthrough curves and assess model parameters. Response surface methodology based on Box–Behnken design was utilized to optimize parameters such as adsorbent mass (6.0–8.0 g), flow rate (0.6–1.0 mL/min), and initial concentration (100–500 μg/g) and to evaluate the interactive effects of the variables on the As (V) adsorption capacity at breakthrough point. Results showed that the optimum As(V) uptake capacity at breakthrough point of 10.57 μg/g could be attained at initial concentration of 418.12 μg/g, CCB mass of 6.6 g, and flow rate of 0.65 mL/min. Based on the analysis of variance, the high value of coefficient of determination ($R^2 \geq 0.9712$) indicates that the quadratic model best describes the experimental data, and the initial concentration is a significant factor on the As(V) adsorption capacity at breakthrough point.

Keywords: Arsenate; Chitosan; Fixed-bed; Box–Behnken design; Yoon–Nelson

1. Introduction

Arsenic is a colorless and odorless metalloid that ranks 20th in natural abundance [1,2]. The presence of arsenic in natural waters is due to the leaching of rocks and minerals such as arsenates, sulfides, sulfosalts, arsenites, silicates, and oxides [3,4]. In surface water and groundwater, arsenic exists in two forms: arsenite, As(III) that predominantly exists as H_3AsO_3 in moderately reducing conditions and arsenate, As(V) that exists mainly as $H_2AsO_4^-$ under oxidizing environment [5–7]. Due to the prevalent contamination of arsenic in surface waters and groundwater and its high toxicity to humans and other organisms, the drinking water standard for arsenic was set at 10 μg/L by the World Health Organization and United

*Corresponding author.

States Environmental Protection Agency [8,9]. Several studies revealed that countries such as Australia, Bangladesh, China, India, Philippines, Taiwan, and Vietnam have high arsenic concentration in their groundwater supplies [8,10]. Long-term ingestion of arsenic-enriched water has been associated with nerve tissue damage, high risk of cancer (bladder, kidney, liver, lung), hyperkeratosis, neuropathy, and black foot disease [9–11]. There are several technologies such as reverse osmosis, oxidation/precipitation, nanofiltration, bioremediation, solvent extraction, and adsorption that are utilized in removing arsenic, specifically As(V), from groundwater [11].

In removing As(III) and As(V) from water, low-cost adsorbents such as alumina nanoparticles in chitosan-grafted polyacrylamide [9], iron oxide-coated cement [12,13], manganese dioxide-coated sand [14], coconut husk carbon [15], activated alumina [16], surfactant-modified chitosan bead [17] have been investigated. Chitosan is one of the most promising adsorbents that have been extensively studied due to its economic viability, safe disposal of spent adsorbent and high metal chelating capacity [17,18]. Recently, several reports focused in utilizing chitosan-coated bentonite (CCB) and chitosan immobilized on bentonite for the removal of Cu(II) [19–22], Ni(II) [21], Pb(II) [21], In(III) [23], and oxidized sulfur compounds [24] from aqueous solution under static conditions. Very few studies determined the use of CCB under fixed-bed conditions, which is commonly utilized in industrial applications. Moreover, results derived from fixed-bed studies could be utilized for the direct application in the remediation of contaminated groundwater using a permeable reactive barrier system [22]. There are no reports available in literature that deals with the optimization of As(V) removal using CCB from actual groundwater under fixed-bed systems. The application of experimental design is essential in order to assess the effect of parameters and their interactions on the adsorption capacity [8].

The main objective of this study is to investigate the removal of As(V) from groundwater using CCB in a fixed-bed system. Specifically it aims to evaluate the effects of initial concentration, adsorbent mass, and flow rate on the fixed-bed adsorption of As(V). Moreover, the optimum operating conditions of the adsorption parameters with respect to adsorption capacity at breakthrough would be determined using response surface methodology (RSM) based on Box–Behnken design (BBD). The dynamics of the optimum fixed-bed adsorption of As(V) on CCB was examined using Thomas and Yoon–Nelson column models.

2. Material and methods

2.1. Reagents and instruments

Low-molecular weight chitosan (75–85% degree of deacetylation) and bentonite ($H_2Al_2O_6S$) were obtained from Sigma-Aldrich. NaOH pellets, concentrated HCl (37% fuming), HNO_3 (65% w/w), arsenic standard (H_2AsO_4 in HNO_3 2–3% 1,000 mg/L As CertiPUR®) and Vitamin C were acquired from Merck (Germany). Sodium arsenate hydrate ($Na_2HAsO_4{\cdot}7H_2O$) and glass wool were procured from Panreac while potassium iodide (weight %: >95) was purchased from Fisher Scientific. Inductively coupled plasma optical emission spectrometry (Perkin Elmer DV2000) was utilized in the quantitative analysis of As(V) residual at a wavelength of 228.812 nm. A peristaltic pump (Masterflex L/S 7518-00) was used in column studies.

Actual groundwater was obtained from a monitoring well located in Chia Nan University of Pharmacy and Science (Tainan, Taiwan). Table 1 illustrates the background values and composition of groundwater utilized in this study.

2.2. Preparation of chitosan-coated bentonite

The procedure utilized in the preparation of CCB was similar to the method by Wan et al. [25]. Chitosan (5.0 g) was dissolved in 300 mL 5% (v/v) HCl and stirred for 2 h at 300 rpm. Then, 100 g bentonite was added into the solution and mixture was stirred for

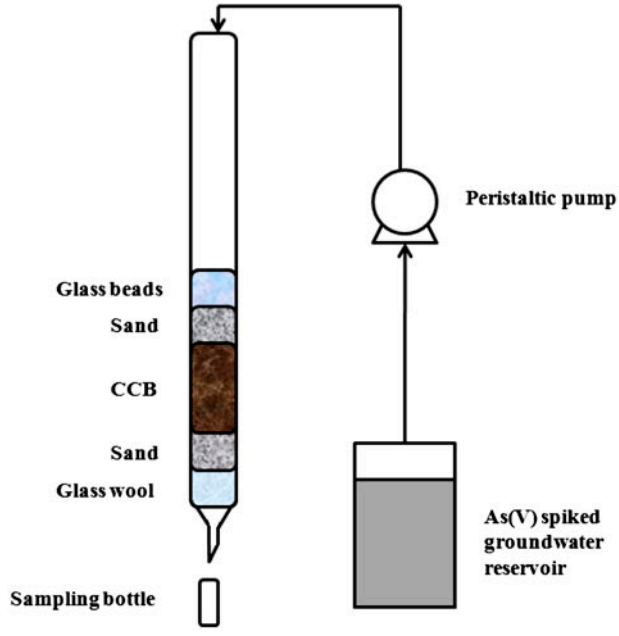

Fig. 1. Fixed-bed setup.

3 h. The addition of 1 N NaOH in a drop wise fashion was carried out until neutralization was achieved. The adsorbent was washed with deionized water and dried in a channel precision oven (DV452 220 V) at 105°C for 24 h. The dried adsorbent was ground and sieved to a particle size of 0.21–0.50 mm.

2.3. Column setup

Continuous adsorption studies were carried out using a borosilicate glass column IWAKI 7740 (internal diameter = 1.9 cm; length = 55 cm) (Fig. 1). The fixed-bed of CCB was underlain with layers of glass wool and sand that serve as support. Moreover, sand and glass beads were added on top of the fixed-bed to regulate and maintain the flow of the influent into adsorbent. The groundwater with known amount of As(V) was pumped into the column in a down flow manner using a peristaltic pump at predetermined flow rate. Throughout the experiment, the inlet solution was maintained at pH 7 since the groundwater pH ranges from 6 to 8. All experiments were carried out under room temperature and atmospheric pressure. The effluent was collected at the bottom of the column at specified time intervals. The effect of parameters such as adsorbent mass, flow rate, and initial concentration were studied to determine the adsorption capacity at breakthrough point of CCB in the removal of As(V).

2.4. Analysis of column data

The column performance is evaluated based on the shape of the breakthrough curve. The breakthrough curve is derived by plotting the normalized concentration (C_t/C_0) against time. Several parameters were computed based on the breakthrough curve. The adsorption capacity at breakthrough (q_b) is describe as when the solute in the effluent reaches 10% of the influent concentration. It is given by Eq. (1) [26]:

$$q_b = \int_0^{V_b} \frac{(C_0 - C_t)\, dV}{M} \tag{1}$$

where V_b is the volume of effluent at breakthrough point (mL), C_0 and C_t are the influent concentration and effluent concentration at time t (mg/L), M is the mass of the adsorbent in the column (g).

The adsorption capacity at exhaustion (q_e) corresponds to the total amount of As(V) contained in the adsorbent bed when the effluent concentration reaches 90% of the influent concentration. It is computed using the equation [26]:

$$q_e = \int_0^{V_e} \frac{(C_0 - C_t) dV}{M} \tag{2}$$

where q_e is the uptake capacity at exhaustion point (mg/g) and V_e is the treated effluent volume at exhaustion (mL).

The total amount of solute or m_{total} (g) sent to the column can be calculated as follows [27]:

$$m_{total} = \frac{C_0 Q t_e}{1000} \tag{3}$$

The total solute removal percentage is computed as follows:

$$Y\ (\%\ \text{removal}) = \frac{m_{ad}}{m_{total}} \times 100 \tag{4}$$

where m_{ad} is the amount of metal retained in the fixed-bed (g). It is derived using numerical integration on the area above the breakthrough curve [27].

2.5. Optimization

The BBD was utilized in evaluating the effect of the operating variables and their combination that will provide the highest adsorption capacity at breakthrough. The method is classified as rotatable or nearly rotatable second-order designs, which uses the three-level incomplete factorial design as its basis [28]. Moreover, BBD requires only 12 runs plus replicates at the center point for a three-factor design. About three levels would be assigned for each factor, which is an essential feature in some experimental situations [28]. In the adsorption of As(V), operating parameters such as initial concentration (100–500 μg/g), flow rate (0.6–1.0 mL/min), and adsorbent mass (6.0–8.0 g) are assigned as independent variables and designated as *A*, *B*, and *C*, respectively. The optimum values were determined by RSM using Design Expert (Version 7.1, Stat-Ease Inc., Minneapolis, USA).

3. Results and discussions

3.1. Effect of adsorbent mass, flow rate, and initial concentration

The breakthrough curves at varying initial concentration, flow rate, and adsorbent mass are shown in Fig. 2. Moreover, Table 2 illustrates the calculated fixed-bed parameters such as breakthrough time (t_b), exhaustion time (t_e), q_b, q_e, and removal efficiency (Y)

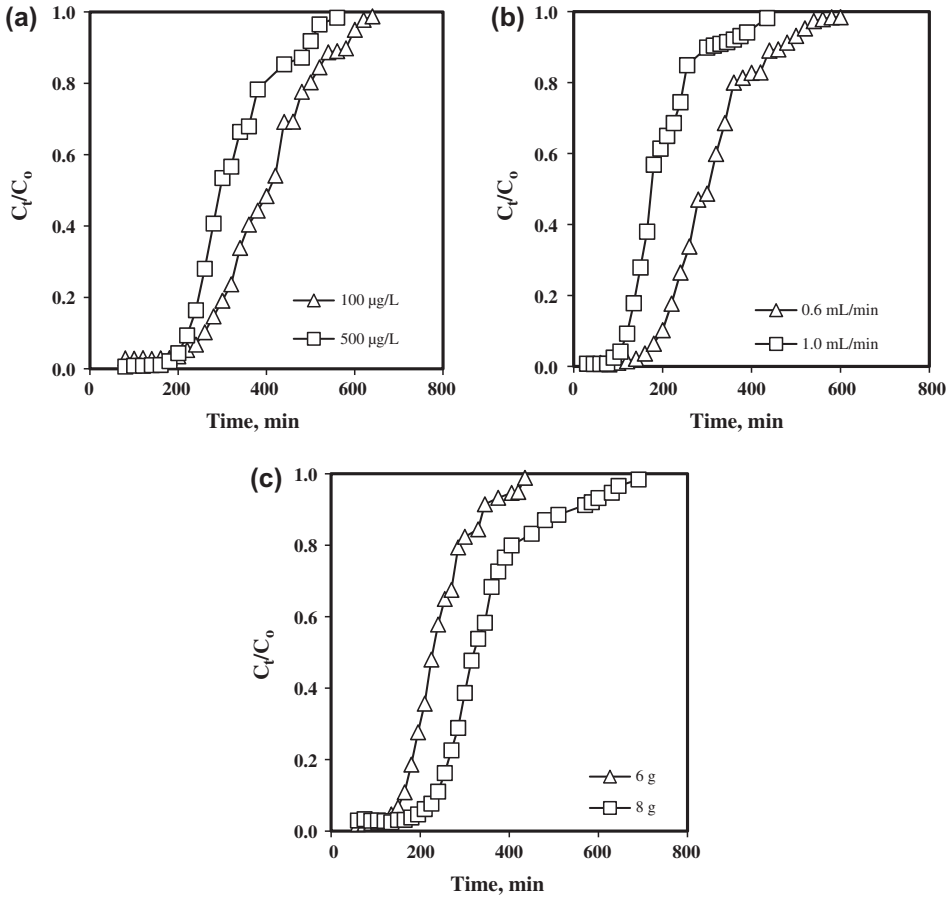

Fig. 2. Effect of (a) initial concentration, (b) flow rate, and (c) adsorbent mass on the breakthrough curve of As(V) adsorption using CCB.

Table 1
Characterization of groundwater from Tainan, Taiwan

Parameters	Unit	Value	Standard
pH	–	8.21	6.0–9.0
Conductivity	µS/cm	88.65	–
Eh	mV	146	–
Dissolved oxygen	mg/L	2.5	–
TOC	mg/L	5.54	–
Turbidity	NTU	16.4	–
Total dissolved solids	mg/L	56.27	1,000
As(V)	µg/L	50.99	50.00
K^+	mg/L	34.39	–
Ca^{2+}	mg/L	24.36	–
Na^+	mg/L	624.9	–
Fe^{2+}	mg/L	0.51	–
Mg^{2+}	mg/L	0.15	–
Cl^-	mg/L	246	250
SO_4^{2-}	mg/L	34.1	–
PO_4^{2-}	mg/L	1.59	–

under varying experimental conditions. In Fig. 2(a), it is observed that the fixed-bed is quickly saturated and shorter t_b and t_e are attained due to high initial As(V)-concentration. On the other hand, an increase in initial concentration caused a corresponding increase in the values of q_b and q_e, which subsequently causes a decline in Y. This is caused by better concentration gradient at high As(V) concentration, which indicates that there is increased mass transfer coefficient or diffusion coefficient [29]. Similarly, Ghosh et al. reported a decrease in the adsorption capacity at breakthrough of arsenic using Mn-incorporated iron (III) oxides when the initial concentration was decreased from 1.00 to 1.72 mg/L [30].

In Fig. 2(b), it was observed that increasing flow rate causes breakthrough curves to become steeper with earlier occurrence of breakthrough and exhaustion times. Moreover, high flow rate values result to lower removal efficiency, q_b and q_e. A high flow rate causes low diffusivity and reduced contact time between As(V) and

Table 2
Influence of varying experimental conditions on the different fixed-bed parameters of As(V) adsorption using CCB

Parameter		t_b (min)	t_e (min)	q_b (μg/g)	q_e (μg/g)	Y (%)
Initial concentration[a] (μg/L)	100	258.57	580.70	3.08	5.06	65.98
	500	221.79	492.01	10.64	16.47	62.85
Flow rate[b] (mL/min)	0.6	198.84	466.79	8.2	2.14	62.81
	1.0	121.32	303.55	7.51	2.09	61.07
Adsorbent mass[c] (g)	6	161.96	337.79	2.99	4.59	66.25
	8	235.36	542.77	3.43	5.33	60.57

[a]Q = 0.6 mL/min; M = 7 g.
[b]C_0 = 300 μg/L; M = 6 g.
[c]C_0 = 100 μg/L; Q = 0.8 mL/min.

CCB, which indicates that there is weak distribution of the solution within the fixed-bed [12,27]. A study on the arsenic removal using natural pozzolan by Kofa et al. showed the same decreasing trend when flow rate was increased from 0.39 to 0.79 cm/min [31].

Fig. 2(c) shows that the breakthrough time and exhaustion time increased with adsorbent mass due to more contact time and better intra-particulate phenomena [12,32]. Moreover, the calculated parameters, such as q_b, q_e, and removal efficiency increased with higher adsorbent mass. This is caused by greater surface area of CCB, which implies that there are more available binding sites for As(V) adsorption [33,34].

3.2. BBD and statistical analysis

The BBD analysis involves a total of 17 runs that were carried out based on a three-factor three-level design. The main objective of the RSM was to determine the regression model to be utilized in describing the adsorption of As(V) using CCB under fixed-bed conditions. A quadratic model was used in determining the relationship between the response and variables. Based on the experimental data, an empirical relationship was obtained that relates the adsorption capacity at breakthrough point to the independent variables and is presented as Eq. (5):

$$X = 8.74 + 4.52A + 0.31B - 0.086C + 0.40AB - 0.26AC + 0.44BC - 0.51A^2 - 0.86B^2 - 0.15C^2 \quad (5)$$

where X is the predicted response (adsorption capacity at breakthrough), and A, B, and C are the coded values for three independent variables such as initial concentration, flow rate, and adsorbent mass, respectively.

In order to check whether the quadratic model employed is adequate and significant, the F-value, p-value, and coefficient of determination (R^2) were obtained. At 95% confidence, the p-value should be less than 0.05 to imply significance. Results show that the low p-value (<0.0001) and high F-value (61.01) indicates that the model is significant in describing the adsorption of As(V) using CCB. The "adequate precision," which measures the signal to noise ratio and a value of greater than 4.0 is desirable, was determined [8]. The value of 23.81 for adequate precision indicates the presence of adequate signal of the model. The coefficient of determination refers to the portion of total variability that can be explained by the model [35]. The closer the value of R^2 to 1.0 and at least 0.80 indicates the goodness of fit of the model. The high value of the derived determination coefficient (R^2 = 0.9712) implies that the quadratic model utilized is best suited in predicting the performance of the adsorption of As(V) with CCB. In Table 3, a good agreement between the predicted and experimental values of q_b is observed, which further validates that the model utilized is significant and adequate.

In Table 4, the summary and results of the analysis of variance (ANOVA) of the experimental design matrix are illustrated. The initial concentration and square effect of the flow rate have significant effect on the As(V) adsorption using CCB. Among the significant factors, initial concentration is highly significant with very low p-value (<0.0001) and high F-value (526.407). This implies that the value of q_b is highly affected by initial concentration. This is attributed to the concentration gradient, which refers to the difference in concentration of the As(V) on the CCB and As (V) present in the solution. It is also the main driving force of adsorption [36].

In Fig. 3(a), the relationship between actual values and predicted values generated by the model is

Table 3
Experimental and predicted values of adsorption capacity at breakthrough of As(V) onto CCB

Run	C_0 (μg/L)	Q (mL/min)	M (g)	Adsorption capacity at breakthrough, q_b (μg/g)	
				Experimental	Predicted
1	100	0.6	7	3.08	2.94
2	500	0.6	7	10.64	11.18
3	100	1.0	7	3.31	2.76
4	500	1.0	7	12.46	12.59
5	100	0.8	6	2.99	3.38
6	500	0.8	6	13.23	12.94
7	100	0.8	8	3.43	3.73
8	500	0.8	8	12.64	12.25
9	300	0.6	6	8.20	7.95
10	300	1.0	6	7.52	7.67
11	300	0.6	8	7.05	6.89
12	300	1.0	8	8.14	8.39
13	300	0.8	7	8.55	8.74
14	300	0.8	7	9.04	8.74
15	300	0.8	7	8.01	8.74
16	300	0.8	7	8.89	8.74
17	300	0.8	7	9.18	8.74

Table 4
The ANOVA results of the surface quadratic model

Source	Sum of squares	df	Mean square	F-value	Prob. > F	Remark
Model	170.4964	9	18.94404	61.03315	<0.0001	Significant
A	163.3911	1	163.3911	526.407	<0.0001	Significant
B	0.755869	1	0.755869	28.45228	0.1626	
C	0.058773	1	0.058773	0.189352	0.6766	
AB	0.629579	1	0.629579	2.028354	0.1974	
AC	0.264969	1	0.264969	0.853666	0.3863	
BC	0.786599	1	0.786599	2.534232	0.1554	
A^2	1.08988	1	1.08988	3.511333	0.1031	
B^2	3.091772	1	3.091772	9.960949	0.0160	Significant
C^2	0.098932	1	0.098932	0.318736	0.5900	

illustrated. It is shown that there is a good agreement between the actual and predicted values, which confirms that the response surface quadratic model utilized in this study is satisfactory in predicting the adsorption capacity at breakthrough time of As(V) using CCB. Meanwhile, Fig. 3(b) shows the 3D surface plot of the interactive effect of flow rate and initial concentration on the adsorption capacity at breakthrough point. As shown, increasing the flow rate from 0.6 to 1.0 mL/min has no significant effect on the adsorption capacity at breakthrough. On the other hand, maximum adsorption capacity at breakthrough point was attained when initial concentration was increased from 100 to 500 μg/g. This shows that the initial concentration has a pronounced effect on the As(V) adsorption that agrees with the ANOVA results in Table 4.

Based from the results, the optimum arsenate adsorption capacity at breakthrough is 10.57 μg/g that is attained under the following conditions: initial As (V) concentration of 448.12 μg/g, flow rate of 0.65 mL/min, and adsorbent mass of 6.6 g. In order to test the validity of the model, four confirmatory runs were performed using the optimum conditions. An average of 10.66 μg/g for As(V) adsorption capacity at breakthrough was obtained, which is similar to the predicted value and falls within the predicted 95% confidence interval of $10.26\ \mu g/g < q_b < 11.87\ \mu g/g$.

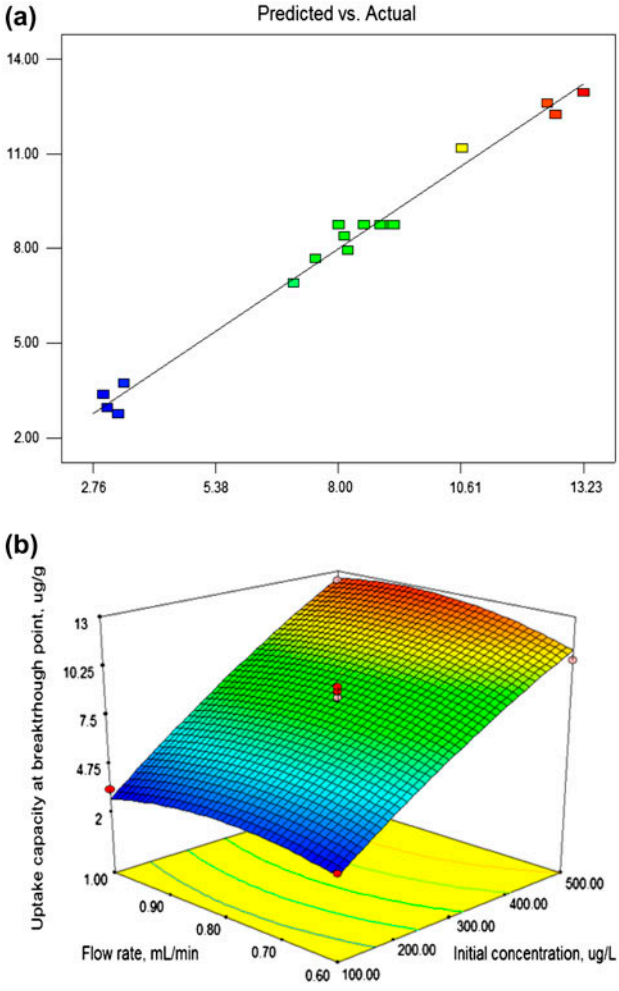

Fig. 3. (a) Correlation between predicted and actual values for the adsorption capacity at breakthrough point of As(V) and (b) response surface plot of uptake capacity at breakthrough point as a function of initial concentration and flow rate.

Overall, this proves that RSM is consistent in the optimization and prediction of the adsorption capacity at breakthrough of As(V) using CCB under fixed-bed system.

3.3. Breakthrough curve modeling

Simple mathematical models are utilized to develop and analyze laboratory-scale fixed-bed studies for the application in the industrial scale [37]. Kinetic column models such as Thomas and Yoon–Nelson are applied to identify the model that would best describe the dynamic behavior of column at optimum condition.

The Thomas model determines the adsorption rate constant of the column and maximum solid-phase concentration of the solute on the adsorbent [12]. The model has the following assumptions: (a) assumes plug flow behavior in the fixed-bed; (b) follows Langmiur kinetics of adsorption–desorption with no axial dispersion; and (c) rate of driving force obeys 2nd order reversible reaction kinetics [38]. The linearized equation of the model is given as Eq. (6):

$$\ln\left(\frac{C_0}{C_t}-1\right)=\frac{k_{\mathrm{Th}}q_0M}{Q}-\frac{k_{\mathrm{Th}}C_0V_{\mathrm{e}}}{Q} \tag{6}$$

where k_{Th} is the Thomas rate constant (mL/min mg) and q_0 refers to the equilibrium As(V) uptake per gram of adsorbent (mg/g) [12].

The Yoon–Nelson model was originally developed to investigate the adsorption and breakthrough behavior of gases on activated charcoal [32]. This model assumes that the rate of decrease in the probability of adsorption for each adsorbate molecule is proportional to the probability of adsorbate adsorption and the probability of adsorbate breakthrough on the adsorbent [34,39]. This model is expressed as Eq. (7):

$$\ln\left(\frac{C_t}{C_0-C_t}\right)=k_{\mathrm{YN}}t-\tau k_{\mathrm{YN}} \tag{7}$$

where k_{YN} is the rate constant (1/min) and τ is the time required for 50% adsorbate breakthrough (min).

Based on the values of the correlation coefficient, both Thomas ($R^2 = 0.9510$) and Yoon–Nelson ($R^2 = 0.9691$) provide to be excellent fit in describing the experimental data. The Thomas model constants k_{Th} and q_0 are obtained with values of 0.03 mL/mg min and 22.64 mg/g, respectively. On the other hand, computed values of the Yoon–Nelson constants are $k_{\mathrm{YN}} = 0.02$ min and $\tau = 291.72$ min.

4. Conclusion

In this work, the removal of As(V) from groundwater using CCB under dynamic conditions was investigated. Results showed that high adsorbent mass, low flow rate and low initial concentration would yield longer time for breakthrough and exhaustion and high removal efficiency. Optimization studies were carried out using BBD to determine the conditions for independent variables such as adsorbent mass, flow rate and initial concentration that would yield the best adsorption capacity at breakthrough point. The maximum adsorption capacity at breakthrough of 10.57 μg/g was attained under the following optimal parameters: initial As(V) concentration of 448.12 μg/g,

flow rate of 0.65 mL/min and adsorbent mass of 6.6 g. Results from ANOVA show that only initial concentration is significant, with low p-value (<0.0001) and high F-value (526.407), which implies that it has a strong effect on the adsorption of As(V) onto CCB. Experimental breakthrough curves were examined using two mathematical models, Thomas and Yoon–Nelson equations. Under the optimum operating conditions, Yoon–Nelson model ($R^2 = 0.9691$) was found to described best the breakthrough curve obtained.

Acknowledgments

The authors would like to thank the Taiwan National Science Council (NSC 99-2221-E-041-017) and Philippine DOST-ERDT scholarship for their financial support.

References

[1] T.D. Çiftçi, E. Henden, Nickel/nickel boride nanoparticles coated resin: A novel adsorbent for arsenic(III) and arsenic(V) removal, Powder Technol. 269 (2015) 470–480.
[2] C.C. Mólgora, A.M. Domínguez, E.M. Avila, P. Drogui, G. Buelna, Removal of arsenic from drinking water: A comparative study between electrocoagulation–microfiltration and chemical coagulation–microfiltration processes, Sep. Purif. Technol. 118 (2013) 645–651.
[3] B.K. Mandal, K.T. Suzuki, Arsenic round the world: A review, Talanta 58 (2002) 201–235.
[4] C.K. Jain, I. Ali, Arsenic: Occurrence, toxicity and speciation techniques, Water Res. 34 (2000) 4304–4312.
[5] S.M. Miller, M.L. Spaulding, J.B. Zimmerman, Optimization of capacity and kinetics for a novel bio-based arsenic sorbent, TiO_2-impregnated chitosan bead, Water Res. 45 (2011) 5745–5754.
[6] S. Tapio, B. Grosche, Arsenic in the aetiology of cancer, Mutat. Res./Rev. Mutat. Res. 612 (2006) 215–246.
[7] M.J. DeMarco, A.K. SenGupta, J.E. Greenleaf, Arsenic removal using a polymeric/inorganic hybrid sorbent, Water Res. 37 (2003) 164–176.
[8] C. Han, H. Pu, H. Li, L. Deng, S. Huang, S. He, Y. Luo, The optimization of As(V) removal over mesoporous alumina by using response surface methodology and adsorption mechanism, J. Hazard. Mater. 254–255 (2013) 301–309.
[9] S. Saha, P. Sarkar, Arsenic remediation from drinking water by synthesized nano-alumina dispersed in chitosan-grafted polyacrylamide, J. Hazard. Mater. 227–228 (2012) 68–78.
[10] T. Hosono, F. Siringan, T. Yamanaka, Y. Umezawa, S. Onodera, T. Nakano, M. Taniguchi, Application of multi-isotope ratios to study the source and quality of urban groundwater in Metro Manila, Philippines, Appl. Geochem. 25 (2010) 900–909.
[11] K. Wantala, E. Khongkasem, N. Khlongkarnpanich, S. Sthiannopkao, K.W. Kim, Optimization of As(V) adsorption on Fe-RH-MCM-41-immobilized GAC using Box–Behnken design: Effects of pH, loadings, and initial concentrations, Appl. Geochem. 27 (2012) 1027–1034.
[12] S. Kundu, A.K. Gupta, As(III) removal from aqueous medium in fixed bed using iron oxide-coated cement (IOCC): Experimental and modeling studies, Chem. Eng. J. 129 (2007) 123–131.
[13] S. Kundu, A.K. Gupta, Analysis and modeling of fixed bed column operations on As(V) removal by adsorption onto iron oxide-coated cement (IOCC), J. Colloid Interface Sci. 290 (2005) 52–60.
[14] S. Bajpai, M. Chaudhuri, Removal of arsenic from ground water by manganese dioxide-coated sand, J. Environ. Eng. 125 (1999) 782–784.
[15] T.S. Singh, K.K. Pant, Equilibrium, kinetics and thermodynamic studies for adsorption of As(III) on activated alumina, Sep. Purif. Technol. 36 (2004) 139–147.
[16] G.N. Manju, C. Raji, T.S. Anirudhan, Evaluation of coconut husk carbon for the removal of arsenic from water, Water Res. 32 (1998) 3062–3070.
[17] M. Sarkar, P. Majumdar, Application of response surface methodology for optimization of heavy metal biosorption using surfactant modified chitosan bead, Chem. Eng. J. 175 (2011) 376–387.
[18] A.J. Varma, S.V. Deshpande, J.F. Kennedy, Metal complexation by chitosan and its derivatives: A review, Carbohydr. Polym. 55 (2004) 77–93.
[19] M.L.P. Dalida, A.F.V. Mariano, C.M. Futalan, C.C. Kan, W.C. Tsai, M.W. Wan, Adsorptive removal of Cu(II) from aqueous solutions using non-crosslinked and crosslinked chitosan-coated bentonite beads, Desalination 275 (2011) 154–159.
[20] N. Grisdanurak, S. Akewaranugulsiri, C.M. Futalan, W.C. Tsai, C.C. Kan, C.W. Hsu, M.W. Wan, The study of copper adsorption from aqueous solution using crosslinked chitosan immobilized on bentonite, J. Appl. Polym. Sci. 125 (2012) E132–E142.
[21] C.M. Futalan, C.C. Kan, M.L. Dalida, K.J. Hsien, C. Pascua, M.W. Wan, Comparative and competitive adsorption of copper, lead and nickel using chitosan immobilized on bentonite, Carbohydr. Polym. 83 (2011) 528–536.
[22] C.M. Futalan, C.C. Kan, M.L. Dalida, C. Pascua, M.W. Wan, Fixed-bed column studies on the removal of copper using chitosan immobilized on bentonite, Carbohydr. Polym. 83 (2011) 697–704.
[23] M.J.C. Calagui, D.B. Senoro, C.C. Kan, J.W.L. Salvacion, C.M. Futalan, M.W. Wan, Adsorption of indium(III) ions from aqueous solution using chitosan-coated bentonite beads, J. Hazard. Mater. 277 (2014) 120–126.
[24] M.C. Lu, M.L. Agripa, M.W. Wan, M.L.P. Dalida, Removal of oxidized sulfur compounds using different types of activated carbon, aluminum oxide, and chitosan-coated bentonite, Desalin. Water Treat. 52 (2014) 873–879.
[25] M.W. Wan, I.G. Petrisor, H.T. Lai, D. Kim, T.F. Yen, Copper adsorption through chitosan immobilized on sand to demonstrate the feasibility for in situ soil decontamination, Carbohydr. Polym. 55 (2004) 249–254.
[26] A. Tor, N. Danaoglu, G. Arslan, Y. Cengeloglu, Removal of fluoride from water by using granular red mud: Batch and column studies, J. Hazard. Mater. 164 (2009) 271–278.

[27] K. Vijayaraghavan, J. Jegan, K. Palanivelu, M. Velan, Removal of nickel(II) ions from aqueous solution using crab shell particles in a packed bed up-flow column, J. Hazard. Mater. 113 (2004) 223–230.
[28] S.L.C. Ferreira, R.E. Bruns, E.G.P. da Silva, W.N.L. dos Santos, C.M. Quintella, J.M. David, J.B. de Andrade, M.C. Breitkreitz, I.C.S.F. Jardim, B.B. Neto, Statistical designs and response surface techniques for the optimization of chromatographic systems, J. Chromatogr. A 1158 (2007) 2–14.
[29] N. Chen, Z.Y. Zhang, C.P. Feng, M. Li, R.Z. Chen, N. Sugiura, Investigations on the batch and fixed-bed column performance of fluoride adsorption by Kanuma mud, Desalination 268 (2011) 76–82.
[30] A. Ghosh, S. Chakrabarti, U.C. Ghosh, Fixed-bed column performance of Mn-incorporated iron(III) oxide nanoparticle agglomerates on As(III) removal from the spiked groundwater in lab bench scale, Chem. Eng. J. 248 (2014) 18–26.
[31] G.P. Kofa, S. NdiKoungou, G.J. Kayem, R. Kamga, Adsorption of arsenic by natural pozzolan in a fixed bed: Determination of operating conditions and modeling, J. Water Process Eng. 6 (2015) 166–173.
[32] S. Chen, Q. Yue, B. Gao, Q. Li, X. Xu, K. Fu, Adsorption of hexavalent chromium from aqueous solution by modified corn stalk: A fixed-bed column study, Bioresour. Technol. 113 (2012) 114–120.
[33] J. Barron-Zambrano, A. Szygula, M. Ruiz, A.M. Sastre, E. Guibal, Biosorption of Reactive Black 5 from aqueous solutions by chitosan: Column studies, J. Environ. Manage. 91 (2010) 2669–2675.
[34] S.S. Baral, N. Das, T.S. Ramulu, S.K. Sahoo, S.N. Das, G.R. Chaudhury, Removal of Cr(VI) by thermally activated weed *Salvinia cucullata* in a fixed-bed column, J. Hazard. Mater. 161 (2009) 1427–1435.
[35] S.M.S. Shahabadi, A. Reyhani, Optimization of operating conditions in ultrafiltration process for produced water treatment via the full factorial design methodology, Sep. Purif. Technol. 132 (2014) 50–61.
[36] Z. Aksu, F. Gönen, Biosorption of phenol by immobilized activated sludge in a continuous packed bed: Prediction of breakthrough curves, Process Biochem. 39 (2004) 599–613.
[37] R.P. Han, L. Zou, X. Zhao, Y. Xu, F. Xu, Y. Li, Y. Wang, Characterization and properties of iron oxide-coated zeolite as adsorbent for removal of copper(II) from solution in fixed bed column, Chem. Eng. J. 149 (2009) 123–131.
[38] H.C. Thomas, Heterogeneous ion exchange in a flowing system, J. Am. Chem. Soc. 66 (1944) 1664–1666.
[39] Y.H. Yoon, J.H. Nelson, Application of gas adsorption kinetics I. A theoretical model for respirator cartridge service life, Am. Ind. Hyg. Assoc. J. 45 (1984) 509–516.